

PROBABILITY FUSION FOR HYPERSPECTRAL AND LIDAR DATA

by

Chiru Ge, Sthandong Normal University, China

Qian Du, Mississippi State University, USA

Presented by: S.Goutham Sai

IITH(CSE)

July 4, 2021

Abstract

In this paper, a new probability fusion strategy is proposed for hyperspectral and LiDAR data classification, which is inspired by the representation residual fusion strategy in our previous works. Unlike the residual fusion strategy which utilizes a collaborative representation classifier, the probability fusion strategy deploys a deep residual network(DRN). This paper compares the two fusion strategies. The experiment results show that the probability fusion strategy with the DRN is better than the residual fusion strategy in classification performance.

Keyterms

Hyperspectral Image

A hyperspectral image is an image which contains the continuous spectrum of every pixel in the image. It is done with the purpose of finding objects, identifying materials, or detecting processes.

LiDAR

LiDAR stands for "laser imaging, detection, and ranging". It is a method for determining ranges (variable distance) by targeting an object with a laser and measuring the time for the reflected light to return to the receiver.

Residual Fusion

Residual fusion is another fusion strategy proposed by the authors in their previous works. It uses the framework of collaborative representation based classification.

Keyterms

Local Binary Pattern

Local binary patterns (LBP) is a type of visual descriptor used for classification in computer vision. LBP is the particular case of the Texture Spectrum model proposed in 1990

Introduction

- Multi-source remote sensing images contain detailed information about the ground. For e.g., LiDAR which contains information about the height and shape information, Hyperspectral Images (HSI) with spectral information.
- HSI and LiDAR images contain complementary information. Hence fusing the two data sources can further improve classification performance.
- However, automatic data fusion is still challenging. This fusion can be achieved by feature level fusion or decision level fusion.
- Many works of the feature level fusion involve the step of dimensionality reduction , which can lead to a feature selection problem.
- To utilize the entire datasets or all features, residual fusion is proposed, which belongs to the decision level fusion.

Introduction

- Inspired by the residual fusion strategy, a novel probability fusion method with the deep residual network(DRN) is proposed which can has the advantage of residual fusion and can achieve higher classification accuracy.
- The main contributions of this paper are:
 - 1 The paper proposes a new method based on probability fusion for the fusion of HSI and LiDAR image.
 - 2 The probability fusion framework can be extended to any spatial features and any deep learning network structures for HSI and LiDAR data fusion.
 - 3 The performance of residual fusion and probability fusion is fairly compared with the previous work on collaborative representation.

Methodology

- In the residual fusion framework, spatial features are first extracted. Spatial features are the stacked features of the Extinction profile(EP) and local binary pattern(LBP) due to their effectiveness.
- Then, the HSI spectral features, HSI spatial features and LiDAR spatial features are normalized because different sources of data generally have different value ranges.
- Next, each source of data is input into a collaborative representation-based classifier with Tikhonov regularization(KCRT) classifier to obtain the residuals.

Tikhonov regularization

Tikhonov regularization, named for Andrey Tikhonov, is a method of regularization of ill-posed problems.

- Finally the residuals are fused to acquire the reconstruction residual that can be used to finalize the class membership of a testing pixel.

Methodology

- Let $r(y) = [r_1(y), r_2(y), \dots, r_l(y), \dots, r_C(y)]$ be the residual vector for a testing sample y , where C is the total number of classes.
- The equation of residual fusion can be written as:

$$r(y) = a r_{HSI}(y) + b(1 - a) r_{HSI_EPLBP}(y) + (1 - b) r_{LiDAR_EPLBP}(y) \quad (1)$$

where a and $b \rightarrow$ weighting parameters,
 $r_{HSI}(y), r_{HSI_EPLBP}(y), r_{LiDAR_EPLBP}(y) \rightarrow$ residual vectors from HSI Spectral features, HSI spatial features and LiDAR spatial features respectively.

- The class label of y can be calculated using:

$$class(y) = \arg \min_{l=1, \dots, C} (r(y)) \quad (2)$$

Methodology

- Let $p(y) = [p_1(y), p_2(y), \dots, p_I(y), \dots, p_C(y)]$ be the probability vector for a testing sample y .
- The equation of residual fusion can be written as:

$$r(y) = cd p_{HSI}(y) + d(1 - c) p_{HSI_EPLBP}(y) + (1 - d) p_{LiDAR_EPLBP}(y) \quad (3)$$

where c and $d \rightarrow$ weighting parameters,
 $p_{HSI}(y), p_{HSI_EPLBP}(y), p_{LiDAR_EPLBP}(y) \rightarrow$ probability vectors from HSI Spectral features, HSI spatial features and LiDAR spatial features respectively.

- The class label of y can be calculated using:

$$class(y) = \arg \max_{I=1, \dots, C} (p(y)) \quad (4)$$

- The advantage of probability fusion and residual fusion is that they both can correct the wrong labels of single-source data. However, both the methods have two sensitive parameters to be tuned.

Methodology

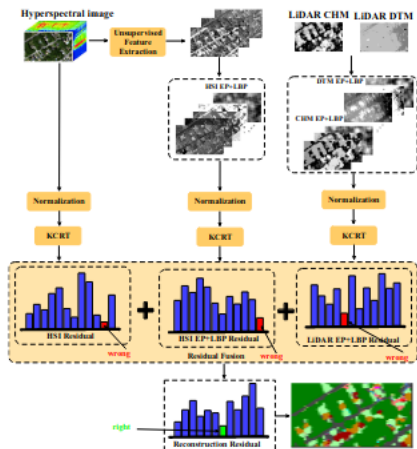


Fig. 1. Representation fusion for HSI and LiDAR data.

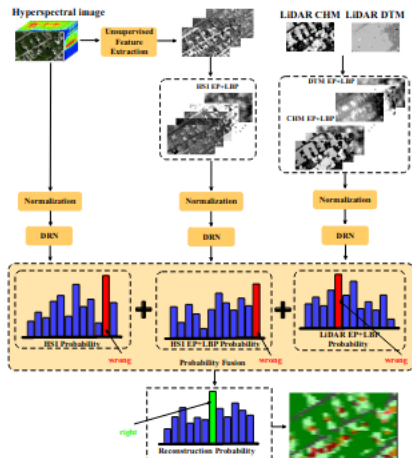


Fig. 2. Probability fusion for HSI and LiDAR data.

Methodology

- 1 Fig. 1 shows a testing sample of the seventh class, which was misclassified by three classifiers utilizing every single source, but accurately classified by the representation residual fusion method.
- 2 Fig. 2 depicts our proposed probability fusion for HSI and LiDAR images, which was inspired by representation residual fusion. The difference is that probability fusion utilizes DRN to classify each source of data, and the testing pixel is assigned to the class with the largest fused probability. DRN acquires the probability matrices of each source. Finally, three probability matrices are fused to obtain the reconstruction probability that can be utilized to finalize the class label of a testing sample.

Experiments

Experiment Data

- Wertheim data come from Goddard's LiDAR, Hyperspectral, and Thermal (G-LiHT) data. The G-LiHT Airborne Imager[6] supplies co-registered LiDAR DTM, LiDAR CHM, LiDAR Point Cloud, hyperspectral reflectance image at 1m spatial resolution and google earth overlay by Keyhole Markup Language (KML) at 0.25m spatial resolution.
- Experiments are conducted on the HSI, CHM and DTM data which were collected in June 2016 across the Wertheim region (geographical coordinate is at $40^{\circ}46'30''$ latitude, $72^{\circ}52'48''$ longitude).
- The hyperspectral image has 114 bands with a spectral range of 420 nm to 950 nm. Spatial resolution of HSI, CHM, and DTM is 1 m. The data set of the entire scene contains 501×1523 pixels.
- There are 5 categories in the Wertheim data. Table 1 shows these categories and the corresponding number of training, validation, and testing samples.

Experiments

	Class	Number of Samples		
No	Name	Training	Validation	Testing
1	Tree	811	969	177163
2	Sea	182	224	10416
3	Sand	130	135	4548
4	Commercial	96	95	1024
5	Pool/Water	50	44	191
6	Major thoroughfares	334	382	4604
7	Bare soil	326	328	6230
8	Road	372	370	6893
9	Parking lot	191	163	1458
10	Grass	296	303	2890
11	Residential grey	116	119	725
12	Residential coffee	144	144	1271
13	Solar panel	30	30	95
14	Car	116	113	420
15	Electric wire	138	140	1052
	Total	3332	3559	218980

Experiments

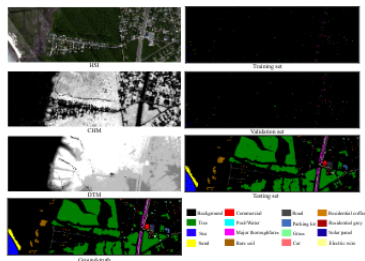


Fig. 3. Wertheim—the HSI data utilizing bands 20, 30 and 40, as blue, green and red respectively; LiDAR CHM image; LiDAR DTM image; Ground-truth; labeled training samples; labeled validation samples; labeled testing samples; the legend of different classes.

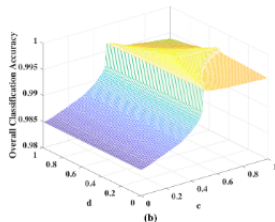
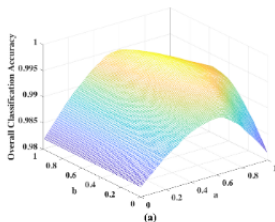
Parameter setting

- Appropriate parameters of KCRT and DRN need to be set. But, due to the limited space, the detailed parameter tuning process of KCRT and DRN is not shown.

Experiments

Parameter setting

- Fig. 4 shows the parameter tuning process for residual fusion and probability fusion.



Experiments

Parameter Setting

- For residual fusion parameters a and b , the optimal parameter are selected through Fig. 4(a): $a = 0.71$ and $b = 0.66$.
- For probability fusion, the best parameters $c = 0.48$ and $d = 0.62$.
- In the experiments, common classification metrics, i.e., AA, OA, Kappa are utilized.

Results

- Table 2 shows classification results of residual fusion. As we can see, residual fusion offers higher classification accuracy than using each individual source, which illustrates the validity of residual fusion.
- Table 3 shows classification results of our proposed probability fusion. As we can see, classification accuracy of probability fusion is higher than that of each source, which illustrates the validity of probability fusion.

Experiments

Results

Table 2. Classification results of residual fusion

	HSI KCRT	HSI_EPLBP KCRT	LiDAR_EPLBP KCRT	Residual Fusion
1	99.92	99.20	99.57	99.99
2	92.59	99.89	99.81	100.00
3	100.00	100.00	98.46	100.00
4	49.80	51.07	100.00	92.29
5	97.38	100.00	96.34	100.00
6	92.72	91.09	85.25	98.00
7	100.00	100.00	99.86	100.00
8	89.57	86.28	79.92	96.27
9	81.07	73.73	76.27	79.63
10	99.24	93.98	73.94	98.51
11	77.38	99.45	98.76	99.59
12	99.61	100.00	99.61	100.00
13	65.26	100.00	100.00	100.00
14	72.62	97.62	98.81	99.05
15	61.03	74.14	99.90	89.07
OA	98.40	98.11	98.15	99.58
AA	85.21	91.10	93.77	96.83
Kappa	0.9530	0.9453	0.9462	0.9877

Table 3. Classification results of probability fusion

	HSI DRN	HSI_EPLBP DRN	LiDAR_EPLBP DRN	Probability Fusion
1	100.00	100.00	100.00	100.00
2	100.00	100.00	98.98	100.00
3	99.98	100.00	95.13	100.00
4	98.51	100.00	100.00	78.42
5	100.00	99.48	97.95	100.00
6	92.90	99.06	84.03	99.52
7	100.00	100.00	99.48	100.00
8	97.39	94.53	96.81	98.94
9	84.25	83.26	93.06	94.31
10	97.04	94.66	71.27	99.79
11	100.00	100.00	100.00	99.31
12	100.00	99.61	84.01	100.00
13	95.00	96.94	100.00	100.00
14	85.28	83.72	41.47	97.62
15	69.21	94.98	79.86	90.11
OA	99.39	99.54	98.48	99.76
AA	94.64	96.42	89.47	97.20
Kappa	0.9820	0.9865	0.9553	0.9929

Experiments

Results

- Compared with Table 2, classification accuracy of probability fusion is higher than that of residual fusion. The reason is that the classification performance of DRN is superior to KCRT.

Table 4. Improvement of classification accuracy by residual fusion and probability fusion

		HSI	HSLEPLBP	LiDAR_EPLBP
Residual Fusion-KCRT	OA	+1.18	+1.47	+1.43
	AA	+11.62	+5.73	+3.06
	Kappa	+0.0347	+0.0424	+0.0415
Probability Fusion-DRN	OA	+0.37	+0.22	+1.28
	AA	+2.56	+0.78	+7.73
	Kappa	+0.109	+0.0064	+0.0376

- Table 4 shows improved classification accuracy by residual fusion and probability fusion, compared with the corresponding counterpart using all the sources.
- Table 4 presents that residual fusion improves classification accuracy more than probability fusion, which demonstrates the potential of residual fusion.

Experiments

Results

- To summarize, residual fusion and probability fusion are both useful for HSI and LiDAR data fusion classification. Although probability fusion with DRN is better than residual fusion with KCRT in performance, residual fusion combined with a better representation classifier may further improve performance.

Conclusion

A new probability fusion strategy is proposed for HSI and LiDAR data fusion. Our proposed probability fusion framework can be extended to any spatial features and any deep learning network structures for HSI and LiDAR data fusion. The experimental results show that the DRN-based probability fusion outperforms the KCRT-based representation residual fusion.